Feasibility of Inertialess Conscan Utilizing Modified DSN Feedsystems

P. D. Potter
Radio Frequency and Microwave Subsystems

The closed-loop conical-scan (conscan) technique has proven to be a useful method for pointing the DSN antennas more accurately than is possible by open-loop methods. As presently implemented, the antenna beam is scanned about the received signal direction by physical movement of the antenna. While straightforward, this approach has at least two disadvantages. Firstly, because of structural distortions, finite angle encoder resolution, and drive servo response, the actual antenna beam direction only approximates the commanded beam direction. Secondly, because of the large mass moved during scan, the rate of scan is severely restricted. If there are significant gain or signal level variations during a scan period, the conscan system interprets these variations as antenna pointing error. Both of these disadvantages would be alleviated in an inertialess conscan system in which the beam scanning was performed electronically. Recently, standard JPL antenna feedhorn software was upgraded (described separately in this report) to calculate, among other things, asymmetric corrugated horn radiation patterns of the type that would be needed for electronic beam scan. A brief look has been taken at the required horn excitation. The results, described in this article, are highly promising.

I. Introduction

The basic conscan technique utilized with the DSN antennas has been described in detail by Ohlsen and Reid (Ref. 1). Basically, the beam is continuously precessed at a specified scan radius about the expected signal arrival direction, and variations of signal are cross-correlated with the beam position. To a first approximation, any error between the precession cone axis and the signal direction results in a sinusoidal variation of the received signal level. This variation may then be processed and utilized to effect a pointing correction. A limitation of conscan is that spacecraft signal level variations and receiver gain fluctuations that occur during one scan period are interpreted as pointing errors; thus it would be desirable to scan very rapidly and integrate over many scan periods, as the spectrum of signal fluctuations tends to decay rapidly with increasing frequency. This objective could be achieved with electronic, rather than mechanical, beam scanning. A second important consideration is that mechanical scanning is inherently limited in accuracy by drive servo response, finite encoder resolution, and structural distortions. To be useful, an electronic beam scanning system would have to be designed such that antenna aperture efficiency and system noise temperature are not significantly degraded by introduction of the beam scanning capability. These prob-

lems are only addressed conceptually in this article, but do not appear serious.

II. Method of Beam Scan

A good way of visualizing the inertialess conscan system is in terms of the more familiar monopulse technique. In the monopulse technique, the feed system produces a "reference" beam (symmetrical with respect to the antenna axis) and a pair of spatially-orthogonal "error" beams (asymmetrical with respect to the antenna axis). For small pointing errors, the error beam signal is directly proportional to pointing error. Each of the two error beams has a plane (containing the antenna axis) of zero output called the "null plane." The two null planes are designed to be as orthogonal as possible, thus providing pointing errors in two perpendicular coordinates.

It can readily be seen from symmetry considerations that if the three outputs from a monopulse feed were combined in such a way that controlled small amounts of the error outputs were added to the reference output, the resultant beam would be scanned off axis by an amount directly related to the amount of error output added to the reference output. Moreover, if the total amount of error signal added to both channels was held constant, but varied sinusoidally and consinusoidally, respectively, with time between the two channels, the result would be a precessing beam; i.e., a conscan. This is the basic concept discussed here. Although we are discussing conical scan and not monopulse, it is convenient to retain the "reference" and "error" nomenclature to identify symmetry properties of feedhorn modes and beams.

Conceptually, the inertialess conscan feed discussed here consists of a corrugated conical horn similar to those presently in use in the DSN, except that capability is introduced in the throat region of the horn for generating a controllable amount of error (asymmetric) mode for beam scan. This generation could be accomplished, for example, by a system of probes driven by semiconductor devices. The feedhorn propagation characteristics of these error modes and their radiation characteristics can be calculated to high accuracy with recently upgraded JPL software (Ref. 2). It turns out that these error modes have very fortunate properties, which appear to have gone unnoticed in previous work; these properties are discussed in the following section.

III. Asymmetric Feedhorn Modes for Beam Scan

The fields inside a corrugated conical feedhorn may be expanded in a series of orthogonal modes (Clarricoats, Ref. 3, has an excellent discussion of this technique), each of which takes the form of a complicated polar (θ) dependence multiplied by sinusoidal/cosinusoidal azimuthal (ϕ) dependence. Additionally, there are two general classes of these "hybrid" modes, designated HE_{mn} and EH_{mn}. Thus the polar and azimuthal electric fields for these modes are given respectively by,

$$E_{\theta_{mn}} = A_n(\theta) \begin{bmatrix} \sin(m\phi) \\ \cos(m\phi) \end{bmatrix} \quad (1a)$$

$$E_{\phi_{mn}} = B_n(\theta) \begin{bmatrix} \cos(m\phi) \\ \sin(m\phi) \end{bmatrix} \quad (1b)$$

The subscript n refers to the order of the Eigenvalue solution to fields in the horn. For the reference beam (as presently used in the DSN feedhorns), the HE_{11} mode is normally used, sometimes in conjunction with the HE_{12} mode for beamshaping purposes. The index m is selected to be 1 for pattern symmetry, and $A_n(\theta)$ is made as nearly equal to $B_n(\theta)$ as possible for polarization purity and high aperture efficiency (see Ludwig, Ref. 4).

Because the corrugated feedhorn has circumferential grooves, it can also support smooth wall modes that have only circumferential wall currents (the TE_{on} modes). Figure 1 shows the minimum three modes necessary to construct circularly-polarized error patterns; namely TE_{01}, EH_{01}/HE_{01}, and HE_{21}.[1] At the horn balance frequency (infinite groove reactance) all three of these error modes have the same Eigenvalue solution and hence propagate with the same velocity (Ref. 3). Additionally, the polar field variation is identical for each. Near the balance frequency, these desirable properties are approximately maintained. Thus, the circularly polarized error beams are inherently broadband. The reference mode does, however, propagate with a different velocity. Thus for the inertialess conscan system described here, the phase of the beam scan is frequency sensitive and must be taken into account.

Using the upgraded hybridhorn program (Ref. 2), HE_{11} (reference), EH_{01}, TE_{01}, and HE_{21} feedhorn 8.415-GHz patterns were computed for the standard DSN horn developed by Brunstein (Ref. 5); these are shown in Figs. 2 through 5. Similar 8.415-GHz patterns were computed for the multifrequency feedhorn recently developed by Williams (Ref. 6); these are shown in Figs. 6 through 9. In all cases, the three

[1] Ludwig's (Ref. 4) proposed definition of normal and cross-polarization is used in Fig. 1.

error mode patterns have essentially coincident phase centers and nearly equal phase delay in travelling from horn throat to aperture. As can be seen in Figs. 2 through 9, all of the error patterns are essentially identical (for a given horn), thus insuring high polarization purity.

IV. Error Mode Excitation and Control

For the standard Brunstein horn, the computed 8.415-GHz mode cutoff horn throat diameter is shown in Table 1 for the lowest modes.

As shown in Table 1, the four required modes have the lowest cutoff diameters, thus allowing rejection of undesired higher order modes.

Figure 10 shows conceptual designs for standard and multifrequency horns with electronic scan.

V. Conclusion

This brief study of beamscan by use of corrugated conical horn modes was performed as a part of the hybrid horn software (Ref. 2) verification process. The results are highly encouraging and indicate that inertialess conscan is feasible with modified versions of present DSN feedhorns. Mode excitation devices have not, however, been investigated.

Acknowledgement

Inertialess conscan and this general method of achieving it was originally suggested by D. A. Bathker of Section 333.

References

1. J. E. Ohlson and M. S. Reid, *Conical-Scan Tracking with the 64-m Diameter Antenna at Goldstone*, Technical Report 32-1605, Jet Propulsion Laboratory, Pasadena, Calif., October 1, 1976.

2. P. D. Potter, "Antenna Feedhorn Software Upgrade," *The Deep Space Network Progress Report 42-51* (this issue).

3. P. J. B. Clarricoats and P. K. Saha, "Propagation and Radiation Behavior of Corrugated Feeds – Part 1. Corrugated Waveguide Feed," *Proc. IEE* (British), Vol. 118, No. 9, Sept. 1971, pp. 1167-1176.

4. A. C. Ludwig, "The Definition of Cross-Polarization," *IEEE Transactions on Antennas and Propagation*, Vol. AP-21, pp. 116-119, January, 1973.

5. S. A. Brunstein, "A New Wideband Feed Horn with Equal E- and H-Plane Beamwidths and Suppressed Sidelobes," in *The Deep Space Network, Space Programs Summary 37-58*, Vol. II, pp. 61-64, Jet Propulsion Laboratory, Pasadena, Calif., July 31, 1969.

6. W. F. Williams, "A Prototype DSN X-S Band Feed: DSS 13 First Application Status," *The Deep Space Network Progress Report 42-44*, Jet Propulsion Laboratory, Pasadena, Calif., pp. 98-103, January and February, 1978.

Table 1. Mode cutoff diameters

Mode	Cutoff diameter, cm (in.)	Comments
HE_{11}	2.29 (0.90)	Normally-used (reference) mode
HE_{21}	3.81 (1.50)	Desired error mode
EH_{01}	4.06 (1.60)	Desired error mode
TE_{01}	4.34 (1.71)	Desired error mode
EH_{11}	5.51 (2.17)	Undesired mode
HE_{12}	5.97 (2.35)	Beamshaping mode

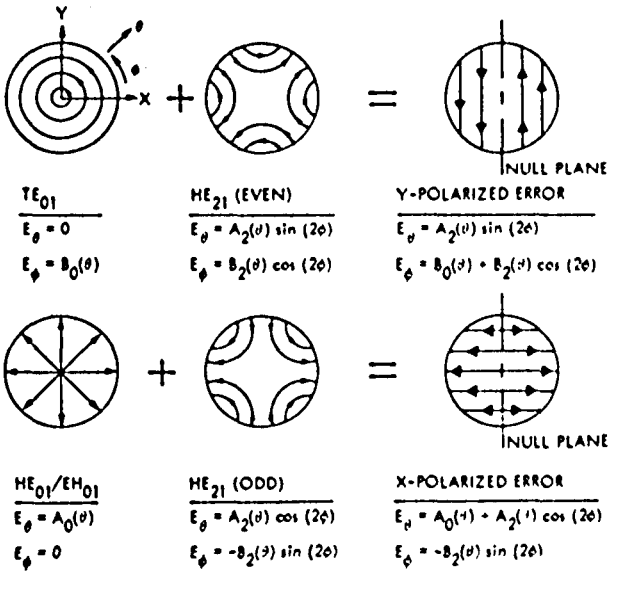

Y-POLARIZED ERROR:

$$E_N = \left\{[B_0(\theta) + B_2(\theta)] + [A_2(\theta) - B_2(\theta)] \sin(2\phi)\right\} \cos\phi$$

FOR $B_0(\theta) = A_2(\theta) = B_2(\theta)$, $E_N = 2B_0(\theta) \cos\phi$ (DESIRED POLARIZATION)

$E_C = 0$ (CROSS POLARIZATION)

X-POLARIZED ERROR:

$$E_N = [A_0(\theta) + A_2(\theta)] \cos\phi + [B_2(\theta) - A_2(\theta)] \sin(2\phi) \sin\phi$$

FOR $A_0(\theta) = A_2(\theta) = B_2(\theta)$, $E_N = 2A_0(\theta) \cos\phi$ (DESIRED POLARIZATION)

$E_C = 0$ (CROSS POLARIZATION)

Fig. 1. Error channel modes in corrugated horns

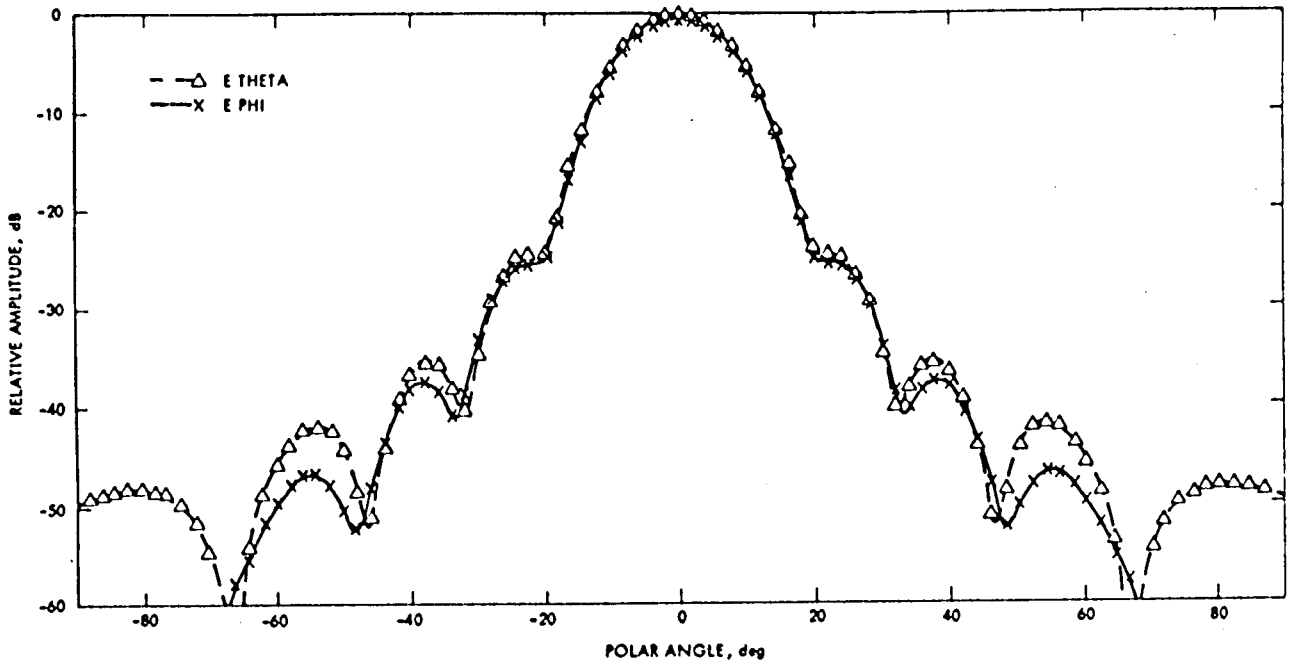

Fig. 2. Brunstein horn, HE_{11} Mode, 8.415 GHz

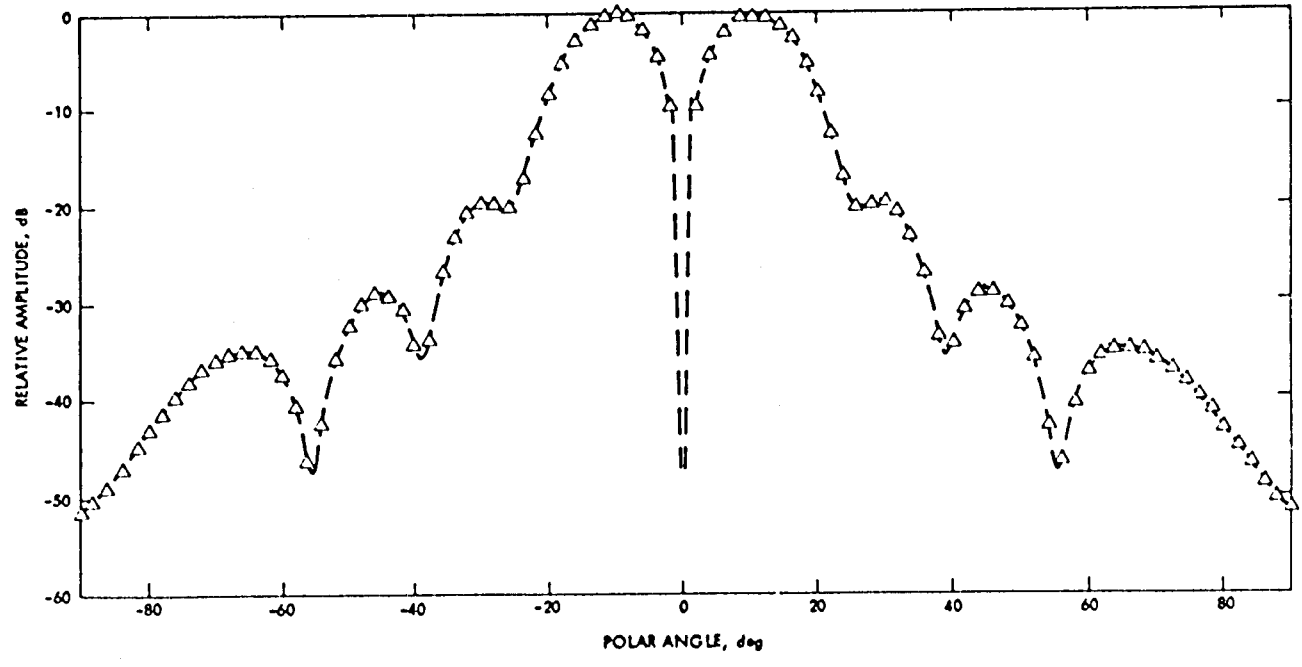

Fig. 3. Brunstein horn, EH_{01} Mode, 8.415 GHz, E theta

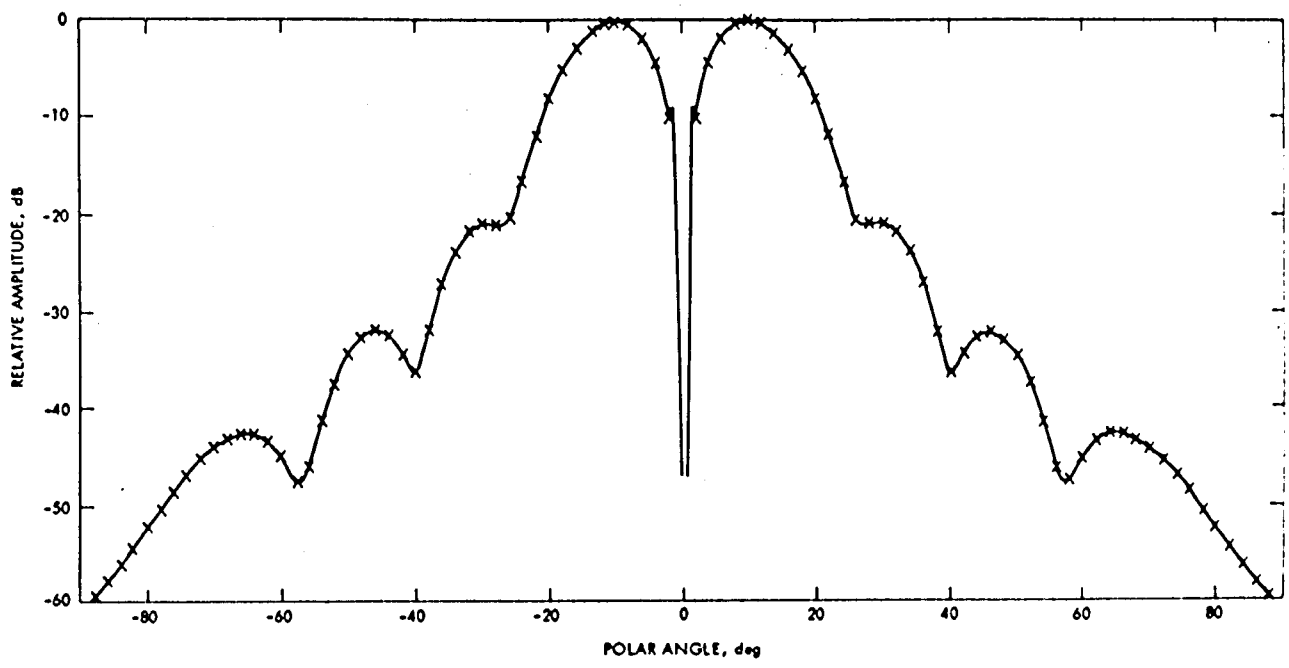

Fig. 4. Brunstein horn, TE_{01} Mode, 8.415 GHz, E phi

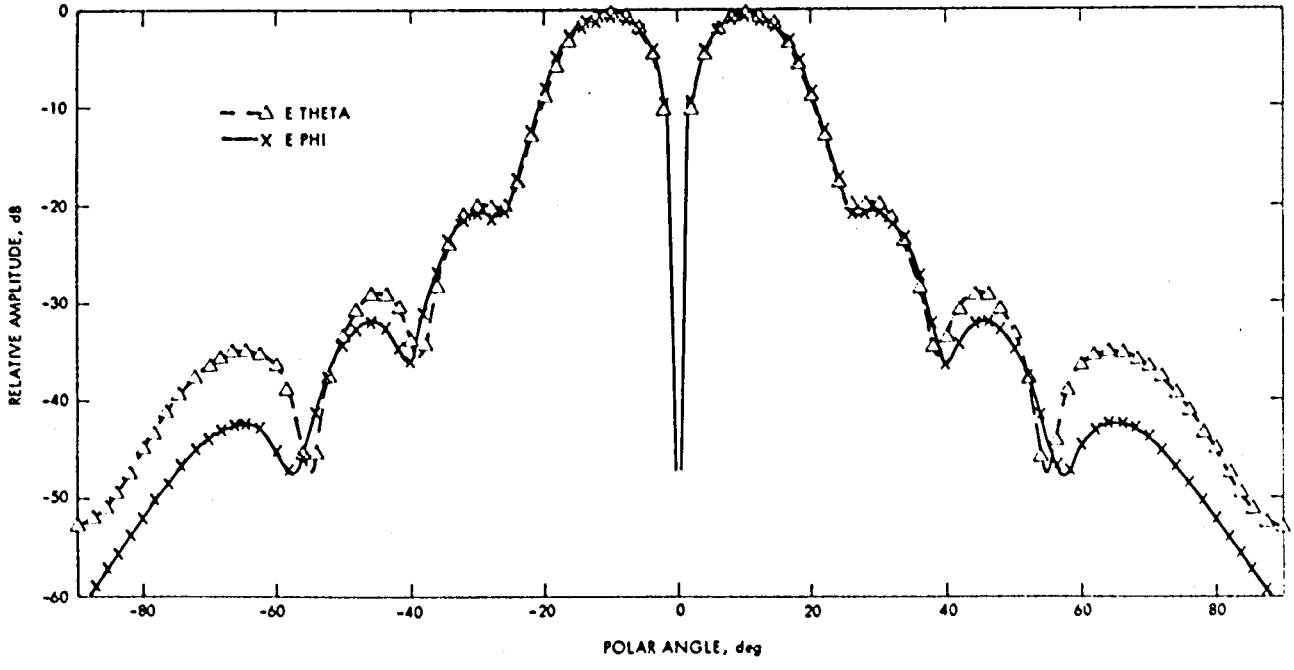

Fig. 5. Brunstein horn, HE_{21} Mode, 8.415 GHz

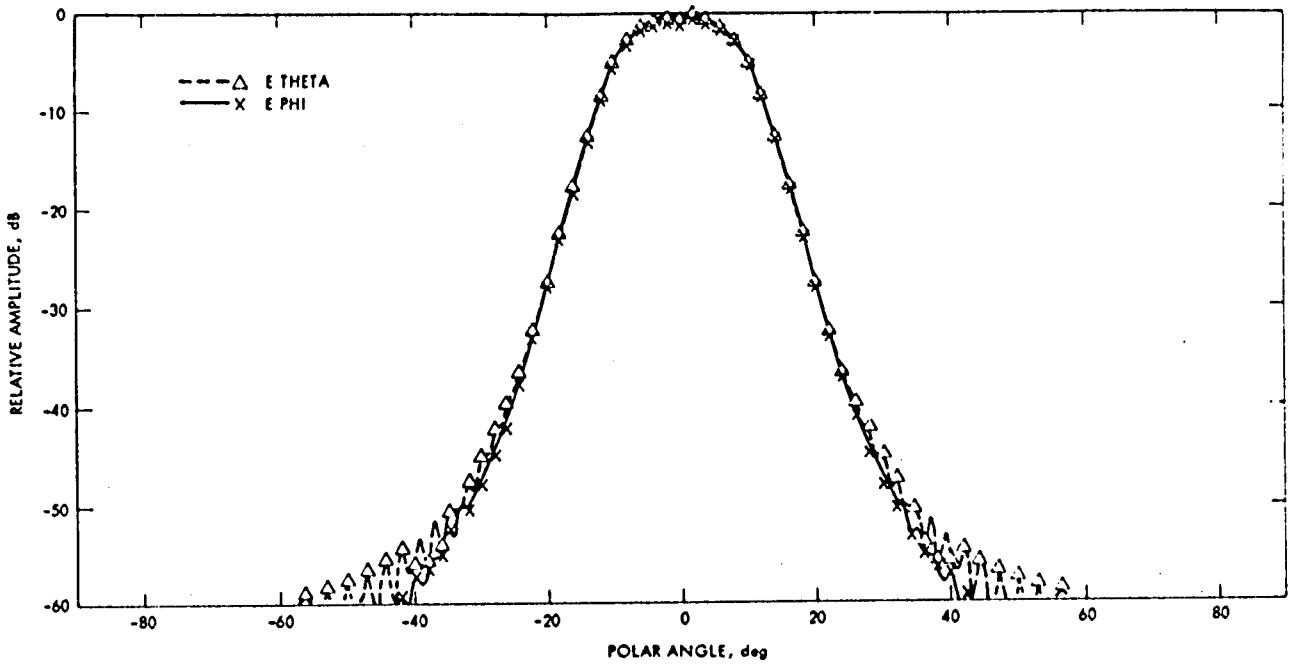

Fig. 6. Williams horn, HE_{11} Mode, 8.415 GHz

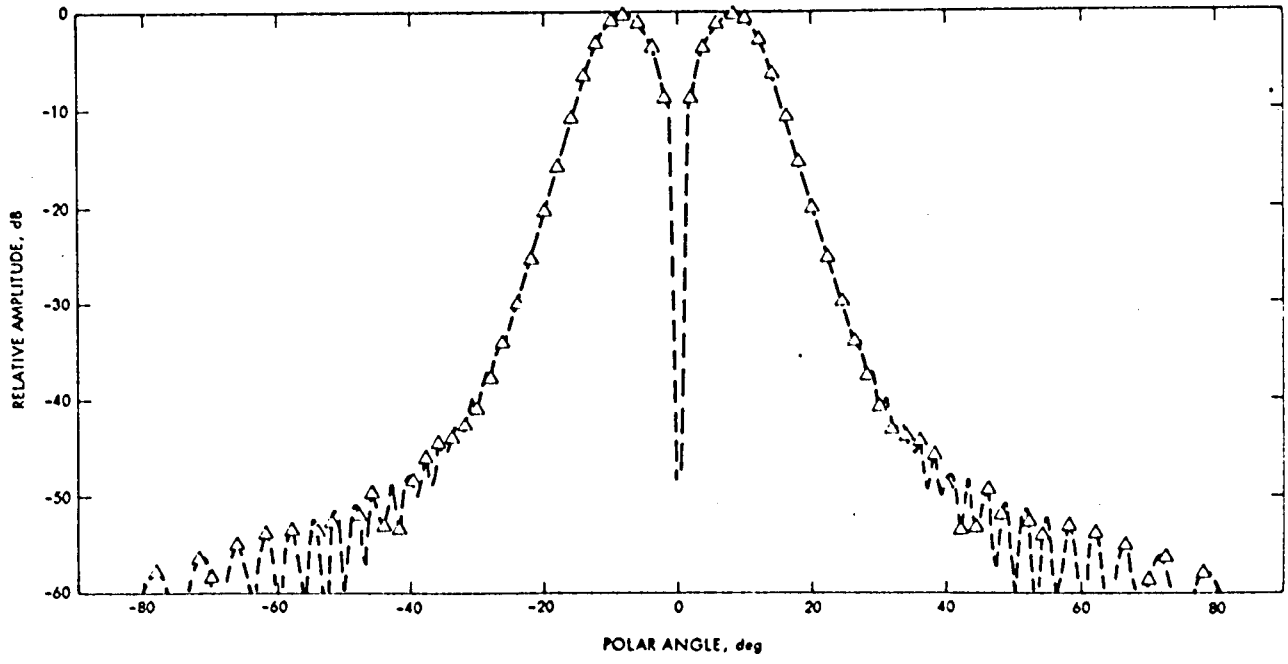

Fig. 7. Williams horn, EH_{01} Mode, 8.415 GHz, E theta

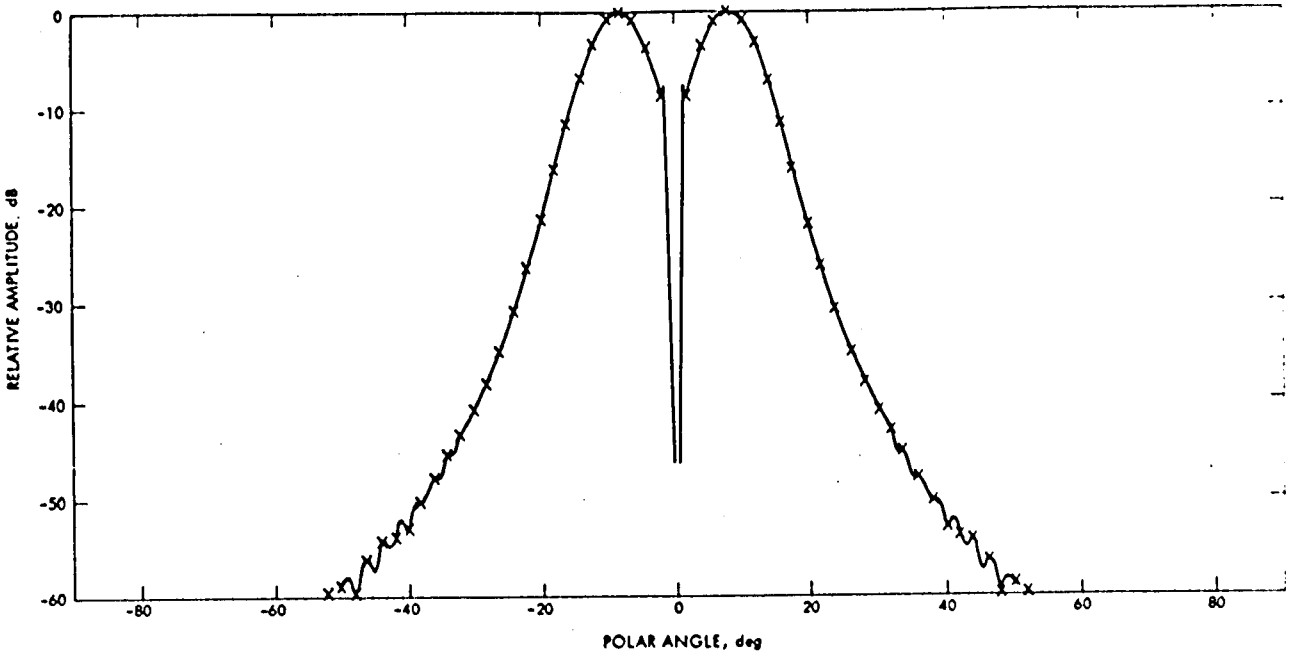

Fig. 8. Williams horn, TE_{01} Mode, 8.415 GHz, E phi

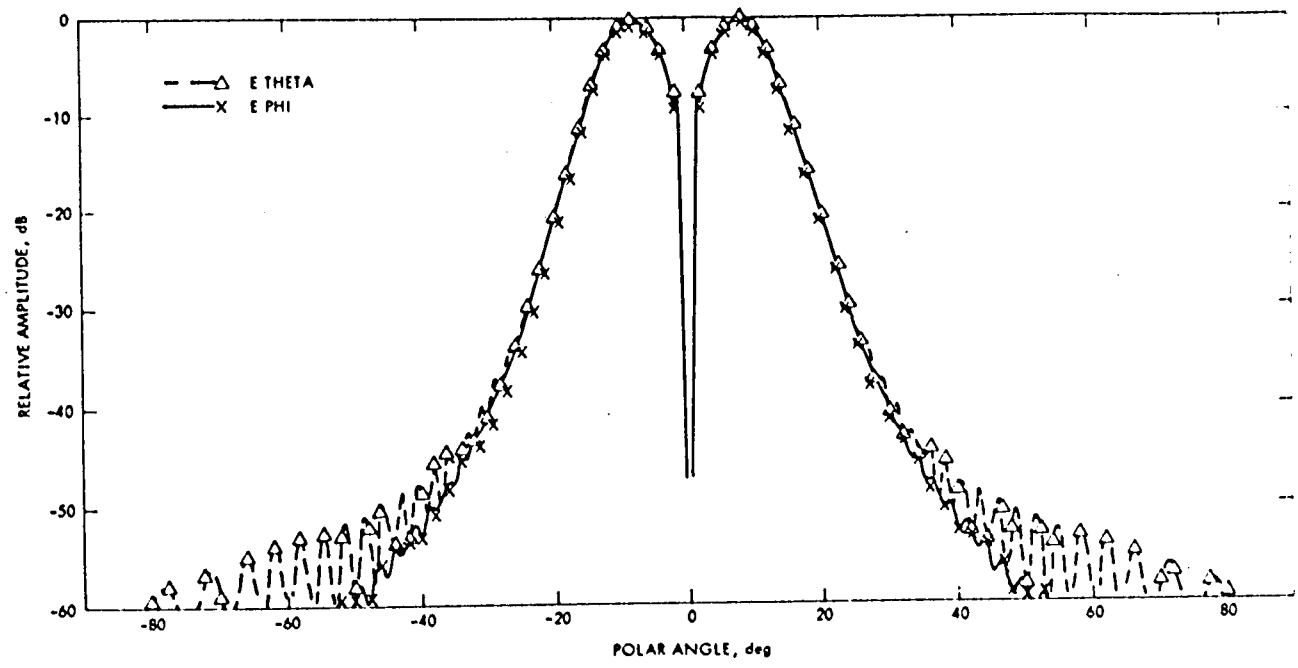

Fig. 9. Williams horn, HE_{21} Mode, 8.415 GHz

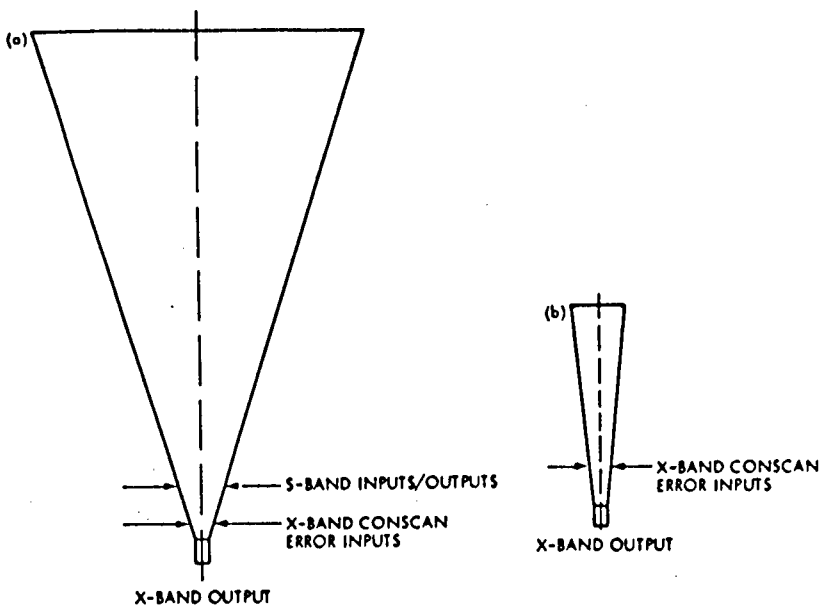

Fig. 10. Conceptual electronic beam scan configurations: (a) multi-frequency horn with electronic X-band beam scan; (b) single-frequency horn with electronic X-band beam scan